


Covalent Attachment of a Rhenium Bipyridyl CO₂ Reduction Catalyst to Rutile TiO₂

Chantelle L. Anfuso,[†] Robert C. Snoeberger, III,[‡] Allen M. Ricks,[†] Weimin Liu,[†] Dequan Xiao,[‡] Victor S. Batista,^{*,‡} and Tianquan Lian^{*,†}

[†]Department of Chemistry, Emory University, Atlanta, Georgia 30322, United States

[‡]Department of Chemistry, Yale University, New Haven, Connecticut 06520-8107, United States

 Supporting Information

ABSTRACT: We have characterized the covalent binding of the CO₂ reduction electrocatalyst ReCOA (Re(CO)₃-Cl(dcbpy) (dcbpy = 4,4'-dicarboxy-2,2'-bipyridine)) to the TiO₂ rutile (001) surface. The analysis based on sum frequency generation (SFG) spectroscopy and density functional theory (DFT) calculations indicates that ReCOA binds to TiO₂ through the carboxylate groups in bidentate or tridentate linkage motifs. The adsorbed complex has the dcbpy moiety nearly perpendicular to the TiO₂ surface and the Re exposed to the solution in a configuration suitable for catalysis.

The development and structural characterization of catalytic materials for selective reduction of CO₂ at low overpotentials is a problem of great technological interest.^{1–4} In recent years, Re(CO)₃Cl(dcbpy) (dcbpy = 4,4'-dicarboxy-2,2'-bipyridine) (ReCOA) and several derivatives have been explored for catalytic reduction of CO₂ to CO.^{5–13} Interestingly, binding of a rhenium bipyridyl complex to TiO₂ electrodes was shown to have increased catalytic reductive ability.¹⁴ However, the configurations of these complexes on TiO₂ and the effect of the surface on catalytic activity have yet to be established. This contribution addresses the nature of the covalent attachment of ReCOA to the TiO₂ rutile (001) surface. We focus on single-crystal TiO₂ since it is an atomically flat, well-characterized surface that is ideally suited for both experimental and theoretical studies.^{15–20} The ReCOA/TiO₂ (001) interface is therefore a model system with many features desirable in an electro- or photocatalytic system and the structural simplicity necessary for rigorous characterization based on spectroscopy and theoretical modeling. By combining sum frequency generation (SFG) spectroscopy and density functional theory (DFT) calculations, we show evidence that ReCOA binds through the carboxylate groups with bidentate or tridentate linkages that orient the dcbpy moiety nearly perpendicular to the surface and expose the Re to the substrate solution as necessary for catalysis.

SFG spectroscopy has been recognized in recent years as a surface selective technique for determining molecular orientation at interfaces.^{21–28} In a typical infrared–visible SFG experiment, two fundamental laser beams of frequency ω_{IR} and ω_{vis} are combined at a surface and generate a resulting sum frequency signal ω_{SF} ($\omega_{\text{SF}} = \omega_{\text{IR}} + \omega_{\text{vis}}$). The efficiency of this process is

enhanced when ω_{IR} corresponds to a vibrational resonance of the interfacial molecule, yielding a vibrational SFG spectrum. For an ordered layer of molecules on a surface, the SFG signal depends on the polarization of ω_{vis} , ω_{IR} , and ω_{SF} with respect to the vibrational and/or electronic transition moment. By monitoring the SFG response as a function of fundamental and generated polarizations, the projection of the transition moment on the laboratory axis can be determined. These results can then be used to screen calculated adsorption geometries. The molecular adsorption geometry at the semiconductor surface can thus be obtained via this synergy of experiment and theory.

In this work, we have investigated the orientation of ReCOA on a rutile TiO₂ (001) single crystal using vibrational SFG spectroscopy in the CO stretching region. The (001) surface was chosen for its C₄ symmetry which simplifies the analysis compared to less symmetric TiO₂ cuts. The details of the experimental setup and sample preparation can be found in the Supporting Information. The black trace in Figure 1 shows the FTIR spectrum of ReCOA on a nanoporous TiO₂ thin film which displays three CO stretching modes: an in-phase symmetric a'(1) stretch at 2040 cm⁻¹, an antisymmetric a'' stretch at 1939 cm⁻¹, and an out-of-phase symmetric a'(2) stretch at 1910 cm⁻¹.²⁹ Also shown is the ReCOA/TiO₂ (001) SFG spectra when $\lambda_{\text{vis}} = 800$ nm ($\lambda_{\text{SF}} \approx 690$ nm) for three different polarization combinations: PPP (indicating the polarization of the sum frequency, visible, and infrared fields, respectively), SSP, and SPS. No discernible signal is seen in either the SSP or the SPS polarization combination for any vibrational modes. The PPP spectrum shows a clear peak at ~ 2040 cm⁻¹, corresponding to the totally symmetric a'(1) stretch, while the two lower frequency modes are absent.

The SFG intensity depends on the product of the IR and Raman cross sections.^{21–24} Raman spectra of related complexes show that all three CO stretching modes are active when the excitation beam is off-resonant with the electronic transition ($\lambda_{\text{ex}} = 1064$ nm). When the excitation beam is near or at resonance, only the a'(1) mode is Raman active.³⁰ The lack of (pre-) resonant Raman activity of the a'' and a'(2) modes has been attributed to the negligible change of equilibrium positions of these normal modes between the ground and the metal(Re)-to-ligand(bpy) charge transfer (MLCT) excited state.³¹ To investigate the extent of resonant enhancement due to the MLCT transition, we have examined the dependence of the SFG spectra

Received: February 13, 2011

Published: April 19, 2011

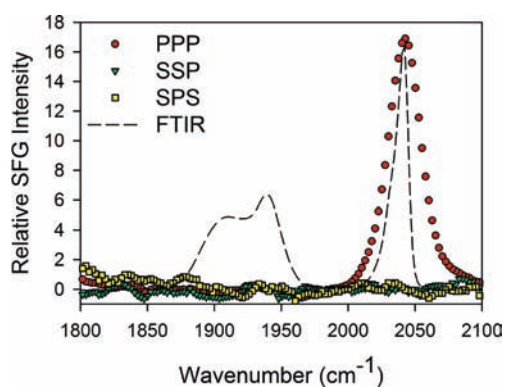


Figure 1. SFG spectra of ReCOA on TiO₂ (001) as a function of ω_{IR} with $\lambda_{\text{SF}} = 690$ nm for three polarization combinations: PPP (red circles), SSP (green triangles), and SPS (yellow squares). Also shown for comparison is the FTIR spectrum of ReCOA on nanoporous TiO₂ (black dashed line).

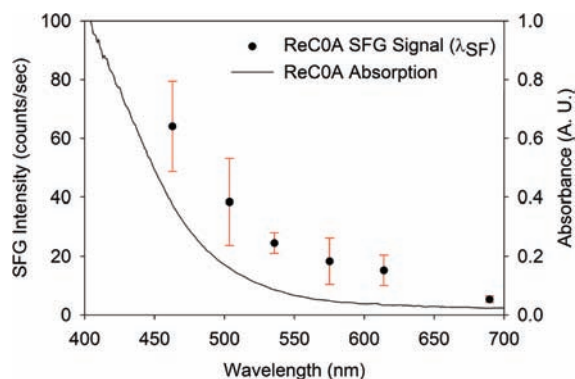


Figure 2. SFG intensity at 2040 cm^{-1} (PPP) as a function of the sum frequency wavelength after correction for grating and CCD efficiencies (black circles, left axis). Also shown is the UV–visible absorption spectrum of ReCOA on nanoporous TiO₂ (solid black line, right axis).

on ω_{vis} . SFG spectra of ReCOA/TiO₂ recorded with $\lambda_{\text{SF}} = 500$ nm also show a lack of intensity of the a'' and $a'(2)$ modes for all polarization combinations (results not shown) and a similar polarization dependence of the $a'(1)$ mode as shown in Figure S1 in the Supporting Information.

Figure 2 shows the UV–visible absorption spectrum of ReCOA on amorphous TiO₂ compared with the SFG peak intensity at 2040 cm^{-1} (PPP) as a function of the sum frequency wavelength. The larger error bars at shorter wavelengths can be attributed to sample degradation which led to variations in peak intensity. There is a clear increase in the SFG signal as the sum frequency approaches the MLCT band at ~ 400 nm, indicating that it is resonantly enhanced, consistent with previous resonant Raman spectra of related complexes.^{30–36}

In order to determine the orientation of ReCOA from the SFG spectra, the SFG response of the $a'(1)$ mode was modeled as a function of orientation angle for the three polarization combinations. In general, the SFG response is given by:^{21,22,37}

$$I(\omega_{\text{SF}}) \propto |\chi_{\text{eff}}^{(2)}|^2 I_{\text{vis}}(\omega_{\text{vis}}) I_{\text{IR}}(\omega_{\text{IR}}) \quad (1)$$

where $I(\omega)$ is the intensity of the given electric field and $\chi_{\text{eff}}^{(2)}$ is the effective second-order nonlinear susceptibility tensor, which is related to individual $\chi_{ijk}^{(2)}$ ($i, j, k = x, y, z$) elements through

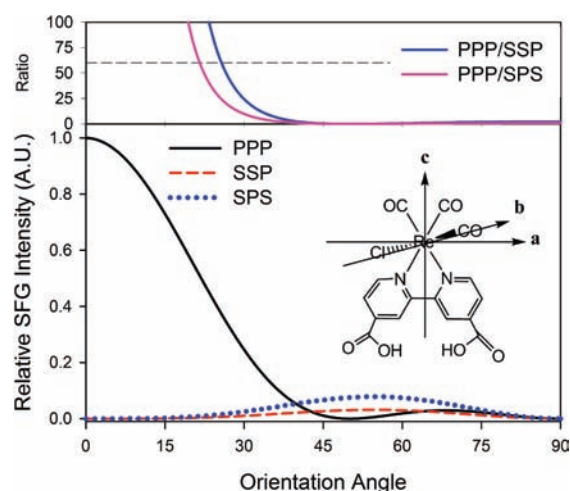


Figure 3. (Lower trace) Model of SFG intensity for the three polarization combinations as a function of the orientation angle: PPP (solid black line), SSP (red dashed line), and SPS (dotted blue line). Inset shows molecular axis system for ReCOA. (Upper trace) Predicted PPP/SSP and PPP/SPS ratios as a function of orientation angle.

Fresnel factors. For a molecule containing a mirror plane on a surface with C_4 symmetry—as in the case of ReCOA/TiO₂ (001)—only four independent nonzero $\chi_{ijk}^{(2)}$ elements remain. The relative values of the nonzero elements are probed using different combinations of input and output polarizations. These elements can be related to the molecular hyperpolarizability $\beta_{\alpha\beta\gamma}^{(2)}$ by transforming from the laboratory frame of reference to the molecular frame:

$$\chi_{ijk}^{(2)} = N_s \sum_{\alpha\beta\gamma=abc} \langle R_{i\alpha} R_{j\beta} R_{k\gamma} \rangle \beta_{\alpha\beta\gamma}^{(2)} \quad (2)$$

where N_s is the molecular number density, R is the rotation transformation matrix element from the molecular coordinate (a, b, c) to the laboratory coordinate (x, y, z), and the angular brackets denotes an ensemble average over possible orientations of the molecule. The molecular axis system for ReCOA is shown in the inset of Figure 3. The c -axis connects the center of the bipyridine to the Re atom (along the direction of the MLCT transition and bisecting the two equatorial CO groups), the b -axis connects the Re center with the axial CO, and the a -axis is perpendicular to b - and c -axes. Assuming a dominant contribution from the MLCT transition to the electronic resonance enhancement, two dominant hyperpolarizability elements are identified for the $a'(1)$ mode: β_{ccc} and β_{ccb} . The details of the orientation analysis are provided in the Supporting Information. Because of the C_4 symmetry of the TiO₂ surface, the β_{ccb} element has no net contribution to the second-order susceptibility.

The lower trace of Figure 3 shows the predicted relative intensities of the SFG signal for the PPP, SSP, and SPS polarization combinations as a function of orientation angle (θ , between the c -axis and surface normal, z or n), while the upper trace displays the predicted PPP/SSP and PPP/SPS ratios of SFG intensities. According to this model the SFG signal in the PPP combination should be dominant at smaller orientation angles (c -axis closer to surface normal), whereas at larger orientation angles all three combinations show appreciable signal. The SFG spectra of ReCOA/TiO₂ (001) show signal for the $a'(1)$ mode only in the PPP combination. As our signal to noise is sufficient to

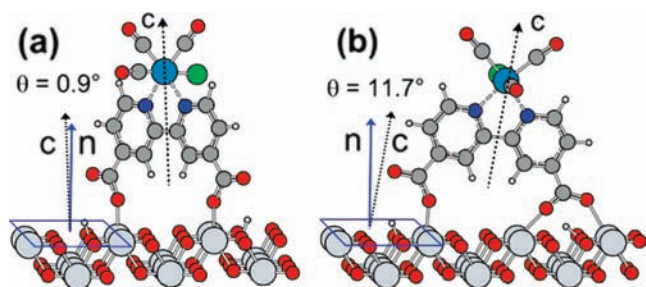


Figure 4. Calculated adsorption geometries for ReCOA on TiO₂ (001). The bidentate (a) isomer is calculated to be 4.85 kcal/mol higher in energy than the tridentate (b) isomer. Color code: H atoms (small white spheres), C atoms (gray spheres), N atoms (blue spheres), O atoms (red spheres), Ti atoms (large light-blue spheres), Cl atoms (green spheres), and Re atoms (large light-blue spheres).

detect a minimum PPP/SPS ratio of 60:1, this analysis yields an orientation angle of $\sim 0\text{--}22^\circ$ from the surface normal.

In support of the experimental work, DFT calculations were performed to obtain an atomistic model of the ReCOA/TiO₂ (001) interface, as described in the Supporting Information. Several possible ReCOA binding motifs were investigated, two of which have orientation angles that lie within the experimentally determined range of $0\text{--}22^\circ$. Both structures bind to the TiO₂ surface by ligation of the carboxylate groups to tetracoordinated Ti centers. Figure 4b depicts the tridentate isomer, which is predicted to be the global minimum and has an orientation angle of 11.7° . The bidentate isomer (4a) is calculated to be ~ 5 kcal/mol higher in energy with an orientation angle of 0.9° . Both structures are energetically equivalent within the assumed error of the DFT level, and it is likely that the SFG signal observed is from a combination of the two isomers.

In conclusion, we have used a combination of SFG spectroscopy and density functional theory to determine the adsorption geometry of the model electrocatalyst ReCOA on a single-crystal TiO₂ (001) surface. SFG spectra of ReCOA/TiO₂ (001) revealed a single vibrational band corresponding to the totally symmetric $a'(1)$ mode. The polarization dependence of this band indicates a molecular orientation angle θ of $0\text{--}22^\circ$ from the surface normal. Two calculated structures displayed orientation angles that fall within the experimentally determined range, resulting from a bidentate ($\theta = 0.9^\circ$) or tridentate ($\theta = 11.7^\circ$) binding linkage of the carboxylate groups to the TiO₂ (001) surface. The upright orientation of ReCOA on TiO₂ leaves the rhenium atom exposed for maximum reductive capacity. This intricate understanding of the binding and orientation of molecules on semiconductor surfaces is essential to advance our understanding of the effect of the surface on catalytic activity and for the design of more efficient and stable catalytic materials.

■ ASSOCIATED CONTENT

S Supporting Information. Details of the computational methods, SFG sample preparation, experimental setup, and SFG polarization analysis. This material is available free of charge via the Internet at <http://pubs.acs.org>.

■ AUTHOR INFORMATION

Corresponding Author

tlian@emory.edu; victor.batista@yale.edu

■ ACKNOWLEDGMENT

V.S.B. acknowledges supercomputer time from NERSC and support from the Division of Chemical Sciences, Geosciences, and Biosciences, Office of Basic Energy Sciences of the U.S. Department of Energy (DE-FG02-07ER15909), and funding for development of computational methods from NSF CHE-0911520 and ECCS-040419. T.L. acknowledges the financial support of Petroleum Research Fund (PRF #49286-ND6) and the U.S. Department of Energy (DE-FG02-07ER-15906).

■ REFERENCES

- (1) Benson, E. E.; Kubiak, C. P.; Sathrum, A. J.; Smieja, J. M. *Chem. Soc. Rev.* **2009**, *38*, 89.
- (2) Underwood, A. J. V. *Ind. Eng. Chem.* **1940**, *32*, 449.
- (3) Balazs, G. B.; Anson, F. C. *J. Electroanal. Chem.* **1993**, *361*, 149.
- (4) Raebiger, J. W.; Turner, J. W.; Noll, B. C.; Curtis, C. J.; Miedaner, A.; Cox, B.; DuBois, D. L. *Organometallics* **2006**, *25*, 3345.
- (5) Hawecker, J.; Lehn, J. M.; Ziessel, R. *J. Chem. Soc., Chem. Commun.* **1984**, 328.
- (6) Hawecker, J.; Lehn, J. M.; Ziessel, R. *Helv. Chim. Acta* **1986**, *69*, 1990.
- (7) Yam, V. W. W.; Lau, V. C. Y.; Cheung, K. K. *Organometallics* **1995**, *14*, 2749.
- (8) Hayashi, Y.; Kita, S.; Brunchwitz, B. S.; Fujita, E. *J. Am. Chem. Soc.* **2003**, *125*, 11976.
- (9) Fujita, E. H. Y.; Kita, S.; Brunchwitz, B. S. In *Proceedings of the 7th International Conference on Carbon Dioxide Utilization*; Park, S.-E.; Chang, J.-S.; Lee, K.-W., Ed.; Elsevier: Seoul, Korea, 2004.
- (10) Fujita, E.; Muckerman, J. T. *Inorg. Chem.* **2004**, *43*, 7636.
- (11) Takeda, H.; Koike, K.; Inoue, H.; Ishitani, O. *J. Am. Chem. Soc.* **2008**, *130*, 2023.
- (12) Smieja, J. M.; Kubiak, C. P. *Inorg. Chem.* **2010**, *49*, 9283.
- (13) Juris, A.; Campagna, S.; Bidd, I.; Lehn, J. M.; Ziessel, R. *Inorg. Chem.* **1988**, *27*, 4007.
- (14) Cecchet, F.; Alebbi, M.; Bignozzi, C. A.; Paolucci, F. *Inorg. Chim. Acta* **2006**, *359*, 3871.
- (15) Diebold, U. *Surf. Sci. Rep.* **2003**, *48*, 53.
- (16) Spittler, M. T.; Parkinson, B. A. *Acc. Chem. Res.* **2009**, *42*, 2017.
- (17) Onda, K.; Li, B.; Zhao, J.; Jordan, K. D.; Yang, J.; Petek, H. *Science* **2005**, *308*, 1154.
- (18) Gundlach, L.; Ernstorfer, R.; Willig, F. *Prog. Surf. Sci.* **2007**, *82*, 355.
- (19) Tisdale, W. A.; Williams, K. J.; Timp, B. A.; Norris, D. J.; Aydil, E. S.; Zhu, X.-Y. *Science (Washington, DC, U. S.)* **2010**, *328*, 1543.
- (20) Duncan, W. R.; Prezhdo, O. V. *Annu. Rev. Phys. Chem.* **2007**, *58*, 143.
- (21) Zhuang, X.; Miranda, P. B.; Kim, D.; Shen, Y. R. *Phys. Rev. B* **1999**, *59*, 12632.
- (22) Rao, Y.; Comstock, M.; Eisenthal, K. B. *J. Phys. Chem. B* **2006**, *110*, 1727.
- (23) Wang, H. F.; Gan, W.; Lu, R.; Rao, Y.; Wu, B. H. *Int. Rev. Phys. Chem.* **2005**, *24*, 191.
- (24) Richmond, G. L. *Annu. Rev. Phys. Chem.* **2001**, *52*, 357.
- (25) Ding, F.; Hu, Z.; Zhong, Q.; Manfred, K.; Gattass, R. R.; Brindza, M. R.; Fourkas, J. T.; Walker, R. A.; Weeks, J. D. *J. Phys. Chem. C* **2010**, *114*, 17651.
- (26) Chen, Z.; Shen, Y. R.; Somorjai, G. A. *Annu. Rev. Phys. Chem.* **2002**, *53*, 437.
- (27) Buchbinder, A. M.; Weitz, E.; Geiger, F. M. *J. Am. Chem. Soc.* **2010**, *132*, 14661.
- (28) Arnolds, H.; Bonn, M. *Surf. Sci. Rep.* **2010**, *65*, 45.
- (29) Asbury, J. B.; Wang, Y.; Lian, T. *Bull. Chem. Soc. Jpn.* **2002**, *75*, 973.
- (30) Waterland, M. R.; Howell, S. L.; Gordon, K. C. *J. Phys. Chem. A* **2007**, *111*, 4604.

- (31) Gamelin, D. R.; George, M. W.; Glyn, P.; Grevels, F.-W.; Johnson, F. P. A.; Klotzbuecher, W.; Morrison, S. L.; Russell, G.; Schaffner, K.; Turner, J. J. *Inorg. Chem.* **1994**, *33*, 3246.
- (32) Waterland, M. R.; Simpson, T. J.; Gordon, K. C.; Burrell, A. K. *Journal of the Chemical Society-Dalton Transactions* **1998**, 185.
- (33) Kleverlaan, C. J.; Stufkens, D. J. *Inorg. Chim. Acta* **1999**, *284*, 61.
- (34) Liard, D. J.; Busby, M.; Matousek, P.; Towrie, M.; Vlcek, A., Jr. *J. Phys. Chem. A* **2004**, *108*, 2363.
- (35) Rodriguez, A. M. B.; Gabrielsson, A.; Motevalli, M.; Matousek, P.; Towrie, M.; Sebera, J.; Zalis, S.; Vlcek, A. *J. Phys. Chem. A* **2005**, *109*, 5016.
- (36) Lewis, J. D.; Clark, I. P.; Moore, J. N. *J. Phys. Chem. A* **2007**, *111*, 50.
- (37) Lambert, A. G.; Davies, P. B.; Neivandt, D. J. *Appl. Spectrosc. Rev.* **2005**, *40*, 103.